Molecular Therapy
Original Article

Transplantation of M2-Deviated Microglia Promotes Recovery of Motor Function after Spinal Cord Injury in Mice

Shuhei Kobashi,[1,2] Tomoya Terashima,[1] Miwako Katagi,[1] Yuki Nakae,[1] Junko Okano,[3] Yoshihisa Suzuki,[3] Makoto Urushitani,[2] and Hideto Kojima[1]

[1]Department of Stem Cell Biology and Regenerative Medicine, Shiga University of Medical Science, Shiga, Japan; [2]Department of Neurology, Shiga University of Medical Science, Shiga, Japan; [3]Department of Plastic Surgery, Shiga University of Medical Science, Shiga, Japan

Despite the poor prognosis of spinal cord injury (SCI), effective treatments are lacking. Diverse factors regulate SCI prognosis. In this regard, microglia play crucial roles depending on their phenotype. The M1 phenotype exacerbates neuroinflammation, whereas the M2 phenotype promotes tissue repair and provides anti-inflammatory effects. Therefore, we compared the effects of M2 and M1 microglia transplantation on SCI. First, we established a method for effective induction of M1 or M2 microglia by exposure to granulocyte-macrophage colony-stimulating factor (GM-CSF) or interleukin (IL)-4, respectively, to be used for transplantation in a SCI mouse model. In the M2 microglia transplantation group, significant recovery of motor function was observed compared with the control and M1 groups. Elevated transcription of several neuroprotective molecules including mannose receptor C type 1 (*Mrc1*), arginase 1 (*Arg1*), and insulin-like growth factor 1 (*Igf1*) was observed. Moreover, intramuscular injection of FluoroRuby dye revealed recovery of retrograde axonal transport from the neuromuscular junction to upstream of the injured spinal cord only in the M2-transplanted group, although the number of migrated microglia were comparable in both M1 and M2 groups. In conclusion, our results indicated that M2 microglia obtained by IL-4 stimulation may be a promising candidate for cell transplantation therapy for SCI.

INTRODUCTION

Spinal cord injury (SCI) is a common traumatic cerebrospinal disease.[1–4] SCI patients suffer from semi-permanent disability and multiple dysfunctions in motor, sensory, and autonomic nervous systems.[3,5] Despite severe impairment of patients' quality of life, treatment options are limited and prognosis is poor.[3,6] Therefore, development of a multifaceted and multidisciplinary SCI treatment[7–15] is a critical unmet need.

The clinical time course of SCI consists of three phases as follows: acute, subacute, and chronic.[16,17] In the subacute phase of SCI, the migration of microglia to the injured site induces an inflammatory response through the release of cytokines such as interferons and interleukins (ILs), leading to activation of their receptors.[18,19] This inflammation is referred to as secondary injury, and it influences the outcome of SCI.[18,19] Therefore, microglia are key players in SCI prognosis and pathogenesis.

Recently, microglia were shown to play a key role in homeostasis of the CNS and pathogenesis of various CNS diseases.[20,21] Microglia have two major phenotypes, known as M1 and M2.[22] M1-type microglia are associated with tissue injury and inflammation, and they recruit inflammatory cells by expressing cytokines such as tumor necrosis factor (TNF)-α and IL-1β.[23–25] Conversely, M2-type microglia regulate tissue repair, anti-inflammatory effects, differentiation of neuronal cells, and proliferation of satellite cells through the expression of IL-4, IL-10, and growth factors such as insulin-like growth factor 1 (IGF1) and transforming growth factor (TGF)-β.[23,24,26] In SCI, inflammation induced by M1-type microglia leads to further damage following primary mechanical injury, whereas the anti-inflammatory cytokines or chemokines secreted by M2-type microglia suppress excessive inflammatory responses and promote regeneration of the injured spinal cord.[27] Therefore, we investigated the therapeutic potential of M2 microglia as a novel candidate for cell transplantation therapy to treat SCI.

Granulocyte-macrophage colony-stimulating factor (GM-CSF) is required to differentiate hematopoietic stem cells and monocyte/macrophage progenitors, which induces the polarization of M1 microglia.[28–30] In contrast, IL-4 produces the opposite effect, including tissue repair and polarization of M2 microglia.[31] We thus separately used GM-CSF or IL-4 to induce M1 or M2 microglia, respectively, in this study. Our results indicate that the transplantation of M2-deviated microglia into the mouse spinal cord was effective in promoting recovery of motor function after SCI.

Received 4 March 2019; accepted 3 September 2019;
https://doi.org/10.1016/j.ymthe.2019.09.004.

Correspondence: Tomoya Terashima, Department of Stem Cell Biology and Regenerative Medicine, Shiga University of Medical Science, Seta Tsukinowa-cho, Otsu, Shiga 520-2192, Japan.
E-mail: tom@belle.shiga-med.ac.jp

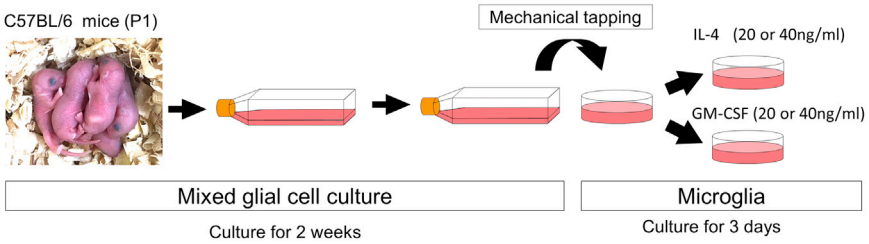

Figure 1. Preparation of Cultured Microglia
The left panel shows the pups at day 1 after birth. After isolating mixed glial cells from their brain cortex, those cells were cultured for 2 weeks. Microglia were collected by mechanical tapping and spread to other culture dishes, followed another 3-day culture with IL-4 or GM-CSF.

RESULTS

Proliferation and Migration of Microglia Cultured with IL-4 or GM-CSF

For *in vitro* experiments, primary microglia were prepared by mechanical tapping after 2-week culture of mixed glial cells from pups 1 day after birth (Figure 1). To examine the proliferative effects of IL-4 and GM-CSF, we cultured microglia with each cytokine at two different concentrations (20 or 40 ng/mL). The number of microglia tended to decrease in 3-day cytokine-free control medium culture. The number of microglia was significantly increased in the presence of IL-4 (20 [IL4-20] or 40 [IL4-40] ng/mL) and GM-CSF (20 [GM-20] or 40 [GM-40] ng/mL), and was most notable in the GM-40 group (Figure 2A). In the GM-CSF group, but not the IL-4 group, microglial proliferation rate was dose dependent (Figure 2A). The migratory ability of these cells was evaluated using a migration assay, which was performed by scratching the bottom of the culture dish containing cells and quantifying the number of cells that migrated to these areas 24 h later. There was a significant increase in migratory capacity in the following order: GM-CSF, IL-4, and no cytokine control (CTR) groups. However, there were no significant differences between the different concentrations within each group (Figure 2B). With regard to phagocytotic ability, the IL4-40 group had significantly lower ability compared with that of the CTR and GM-40 groups. The GM-40 group showed the highest phagocytic ability among the three groups (Figure 2C).

Immunocytochemistry of Microglia with IL-4 or GM-CSF *In Vitro*

Isolated microglia were incubated with IL-4 or GM-CSF for 3 days. Immunocytochemistry was performed for CD86 as an M1 marker and CD206 as an M2 marker to evaluate polarization effects of each cytokine. CD86 staining was observed in approximately 40% of the microglia in the GM-40 group, and was significantly different compared with that for the CTR group (cytokine-free medium) (Figure 3A). However, no significant difference was observed in GM-20 (GM-CSF 20 ng/mL) and two IL-4 groups when compared with the CTR group (Figure 3A). CD206 expression was significantly elevated in IL4-20 and -40 (IL-4 20 and 40 ng/mL) groups compared with the CTR group, and most microglia showed CD206 in these groups. In contrast, no significant elevation was observed in the two GM-CSF groups (Figure 3B).

mRNA Expression of Microglia Cultured with IL-4 or GM-CSF

After incubation of isolated microglia for 3 days with IL-4 or GM-CSF, mRNA expression of *Cd86*, mannose receptor C type 1 (*Mrc1*) coding CD206, and nitric oxide synthase (*Nos)2*, which are known to be elevated in M1 microglia, and arginase 1 (*Arg1*), which is typically upregulated in M2 microglia, were analyzed by qRT-PCR. *Cd86* expression was significantly increased in the GM-40 group compared with the CTR group (no cytokine), similar to the results of immunostaining (Figure 4). *Mrc1* expression was significantly increased in both IL4-20 and IL4-40 groups, but this effect was not dose dependent. A significant elevation in *Nos2* expression was observed in the GM-40 group. *Arg1* expression was significantly increased in both IL4-20 and IL4-40 groups and to similar levels (Figure 4). As shown in *in vitro* studies above, we identified selective polarization to M1 or M2 microglia, which was used in subsequent cell transplantation experiments for SCI.

Cell Transplantation Therapy with Microglia for SCI: Improvement of Motor Function with Cell Transplantation

The SCI mice model was prepared by nuclear excision of right spinal cord tissue with a 1-mm-diameter skin biopsy puncher (Figure 5A). M1 microglia incubated with GM-CSF (40 ng/mL) and M2 microglia incubated with IL-4 (40 ng/mL) were separately mixed with Matrigel and administered to the injured spinal cord site in the SCI mice model. Recovery of motor function was evaluated using the Basso mouse scale (BMS) and hindlimb reflex scoring (Figures 5B and 5C). BMS results indicated that all groups showed recovery of motor function until day 28 after injury. Among groups, recovery was significantly better in the M2 group than in the M1 and control Matrigel only (CTR) groups (Figure 5B). As for hindlimb reflex scoring, a significant improvement was observed in the M2 group when compared with the CTR group in the fourth week (Figure 5C). The effect of injection time of M2 microglia was evaluated by the transplantation on day 0, 3, or 7 after SCI. It was shown that the recovery of motor function in the day 0 group was superior to day 3 and day 7 groups (Figure 5D and 5E). Overall, movement in the M2 group was better than the CTR and M1 groups (Videos S1, S2, and S3), with rapid movement and absence of claudication in the M2 group (Video S3).

The advantage of M2 microglia transplantation compared with systemic administration of IL-4 was also investigated. BMS and hindlimb reflex scoring were significantly recovered in the M2 group compared with IL-4 systemic injection (Figures 5F and 5G).

Tissue Repair of Spinal Cord with Cell Transplantation

Spinal cord sections of mice 4 weeks after SCI and cell administration were evaluated immunobiologically. Staining with β3-tubulin, a neuronal marker, showed fibrous components of neurons at the

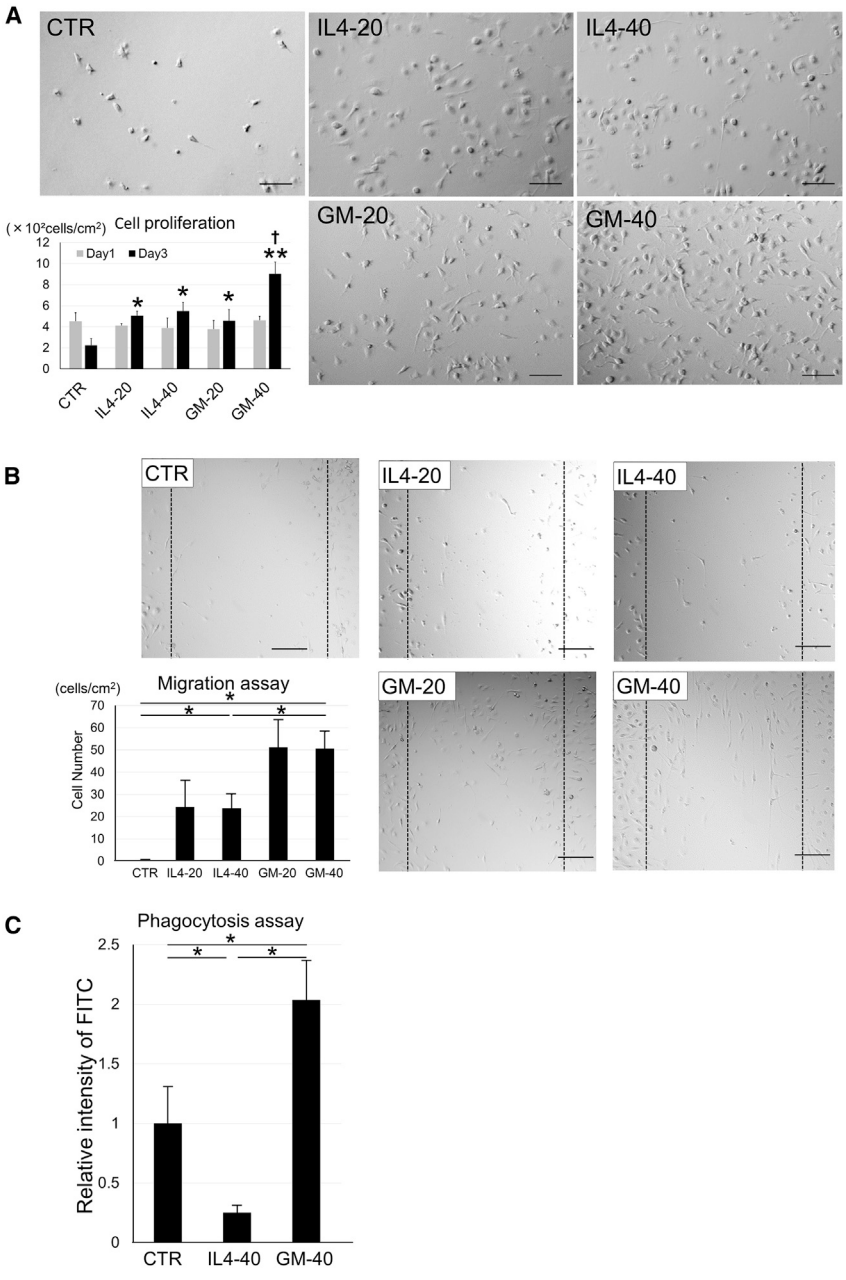

Figure 2. Proliferation, Migration, and Phagocytosis of Microglia Cultured with IL-4 or GM-CSF

(A) Phase-contrast micrographs of microglia cultured with IL-4 (20 [IL4-20] or 40 [IL4-40] ng/mL) or GM-CSF (20 [GM-20] or 40 [GM-40] ng/mL). Graphs show cell number of microglia ($\times 10^2$ cells/cm^2) on days 1 and 3. Error bars showed means + SD (n = 3 in each group). *p < 0.05 as compared with day 3 control group; †p < 0.01 as compared with day 3 other groups. (B) Micrographs and migration assay of microglia. After 3-day culture with none (CTR), IL-4 (20 [IL4-20] or 40 [IL4-40] ng/mL), or GM-CSF (20 [GM-20] or 40 [GM-40] ng/mL), migration assay was performed. Photographs were taken 12 h after scratching. Broken lines show scratched area in each group. Graphs show number of migrated cells to scraped area. Error bars showed means + SD (n = 3 in each group). *p < 0.05. (C) Phagocytosis assay of microglia in IL4-40 and GM-40 groups on day 3. FITC intensity of microglia were calculated for each group. Bars showed mean + SD (n = 3 in each group). *p < 0.05. Scale bars, 100 μm. CTR, no cytokine control group.

SCI and injection sites, but no obvious neuronal cell bodies were observed (Figure 6A). The fluorescence intensity of the same site was also quantified in each group, but no significant difference was observed among three groups (Figure 6B).

Immunohistochemical staining with the astrocyte markers, glial fibrillary acidic protein (GFAP) and glutamate transporter-1 (GLT-1), were also performed in the injured spinal cord from CTR, M1, and M2 groups (Figure 6A; Figure S1). Although there was some GFAP-positive staining around the Matrigel injection site, there was no staining in most of the injured lesions in all three groups (Figure 6A). Quantitative analysis of GFAP and GLT-1 staining at the injury site did not show any significant differences among groups (Figure 6B; Figure S1).

Numerous Iba-1-positive cells (a microglial marker) were observed in the Matrigel injection site (Figure 6A). In contrast with β3-tubulin and GFAP, the cell numbers were significantly increased in the M1 and M2 microglia-administered groups compared with the CTR group (Figure 6B). In addition, CD86 and CD206 immunostaining in the transplanted site of the spinal cord revealed that the intensity of CD86 staining was significantly lower in the M2 group than in others, whereas CD206 was significantly higher in the M2 group (Figure 6C).

Next, we transplanted microglia prepared from GFP mice into the SCI model and investigated residual GFP-positive cells on 7, 14, and 28 days, to analyze the fate of transplanted microglia in the injured spinal cord (Figure S2). Although GFP-positive cells were observed on days 7 and 14 in the injured spinal cord, these cells were hardly detectable on day 28 (Figure S2).

Analysis of mRNA Expression in the Spinal Cord with Cell Transplantation

RNA was extracted from the mouse spinal cord 4 weeks after SCI and cell transplantation, and gene expression analysis was performed for CD antigens, nitric oxide-related enzymes, and growth factors in CTR, M1, and M2 groups. mRNA expression of the M1 markers, *Cd86* and *Nos2*, was not significantly different among groups.

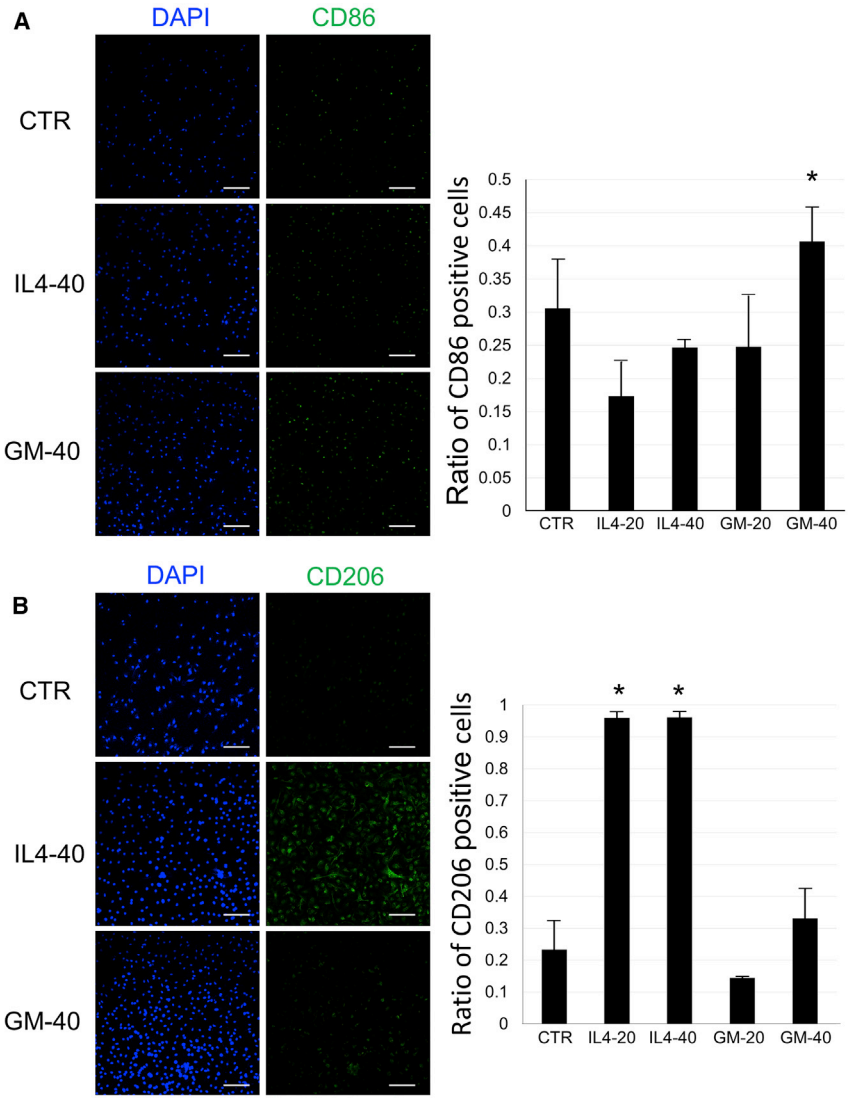

Figure 3. Immunocytochemistry of Microglia after Incubation with IL-4 or GM-CSF

(A) Immunocytochemistry with CD86 antibody (as a M1 marker) in the CTR, IL-4 (20 [IL4-20] or 40 [IL4-40] ng/mL), or GM-CSF (20 [GM-20] or 40 [GM-40] ng/mL) group on day 3. Left panels show DAPI (nuclei: blue) and CD86 staining (green) in microglia from CTR, IL4-40, and GM-40 groups. Right bar graph shows the ratio of CD86-positive microglia. Error bars showed means + SD (n = 3 in each group). (B) Immunocytochemistry with CD206 antibody (as a M2 marker) in the CTR, IL4-20, IL4-40, GM-20, or GM-40 group on day 3. Left panels show DAPI (nuclei: blue) and CD206 staining (green) in microglia from CTR, IL4-40, and GM-40 groups. Right bar graph shows the ratio of CD206-positive microglia. Scale bars, 100 μm. Error bars showed means + SD (n = 3 in each group). *$p < 0.05$ as compared with the CTR group. CTR, no cytokine control group.

Expression of M2 markers, *Mrc1* and *Arg1*, was significantly increased in the M2 group compared with CTR and M1 groups. In addition, *Igf1* expression was also examined as a representative growth factor, and it was significantly increased in the M2 group compared with the CTR and M1 groups. However, there was no significant difference in the expression of brain-derived neurotrophic factor (*Bdnf*) among groups (Figure 7).

Recovery of Axonal Transportation with Cell Transplantation

Axonal transportation was examined using retrograde tracer (FluoroRuby) in SCI mice, 4 weeks after treatments. FluoroRuby was injected into hamstrings on the injured side of the spinal cord. Five days later, sections were cut at the spinal (L1), proximal (Th13), and distal (L2) levels of the injured site (Figure 8A). In axial sections of the spinal cord, at the distal level (L2) of SCI, FluoroRuby-positive neurons were observed at the anterior horn of the spinal cord in CTR, M1, and M2 groups (Figure 8B, left upper panel in each group). The number of positive cells was not significantly different among the groups (Figure 8C, upper). At the injured level of the spinal cord, FluoroRuby-positive staining was widely observed in all three groups (Figure 8B, left lower panel in each group). In contrast, some FluoroRuby-positive neurons were clearly observed at the anterior horn of the injured side in the proximal spinal cord only in the M2 group, but not in the CTR and M1 groups (Figure 8B, right panels in each group). The number of positive cells at the proximal levels of the spinal cord was highest in the M2 group (Figure 8C).

DISCUSSION

Both M1 and M2 microglia are implicated in the pathogenesis of various neurological diseases.[32–34] The population and the proportion of M1 and M2 microglia are reported to change dynamically depending on disease states.[35] For example, in amyotrophic lateral sclerosis (ALS) and Alzheimer's disease, the initial M2 environment in the spinal cord or brain gradually alters into M1 milieu as the disease progresses.[23,36–38] In SCI, the infiltration of M2 cells to the injury site occurs temporarily in the acute or subacute phase; conversely, the M1-dominant environment is sustained for a long time.[27,39] Several reports showed that the reduction of M1 and/or increase of M2 microglia in recipient mice with SCI by drug administration and IL-4 systemic injection augments the effects of treatment, suggesting that the balance of M1/M2 microglia is crucial.[40–42] M2 microglia is further divided into three subclasses, M2a, M2b, and M2c. M2a microglia is a most classical phenotype of M2, and it is induced by IL-4 stimulation.[43] Moreover, the M1/M2 paradigm is recently going to shift from an M1/M2 binary system to a spectrum of activity.[24] It should be noted that over 90% of IL-4-induced M2 microglia expressed CD206, and approximately 20% of the M2 microglia expressed CD86 by *in vitro* immunostaining in this study. This result

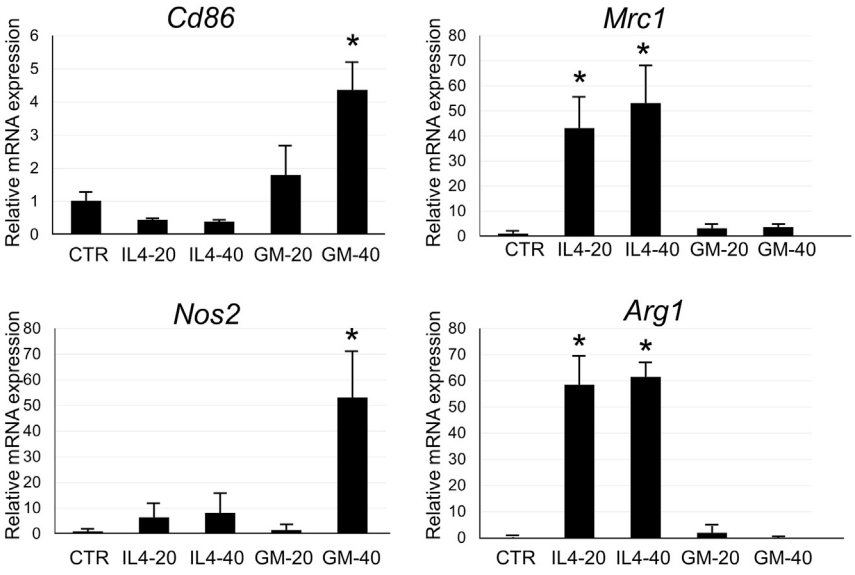

Figure 4. mRNA Analysis in Microglia after Incubation with IL-4 or GM-CSF

Analysis of mRNA gene expression in cultured microglia in CTR (no cytokine buffer control), IL-4 (20 [IL4-20] or 40 [IL4-40] ng/mL), or GM-CSF (20 [GM-20] or 40 [GM-40] ng/mL) on day 3. Bar graphs show the relative mRNA expression of *Cd86*, *Mrc1*, *Nos2*, and *Arg1* in microglia against the CTR group. These mRNA expressions were normalized to that of β-actin. Error bars showed mean + SEM (n = 3 in each group). *$p < 0.05$ as compared with the CTR group.

suggests that a certain population of the M2 microglia expressed the M1 marker. Co-expression of M1 and M2 markers seems to be inconsistent. However, the presence of double-positive microglia for CD86 and CD206 has been reported in a previous article, which is interpreted as a transition state from M1 to M2.[44] Although the M1/M2 paradigm might not precisely profile the phenotypes as inflammatory or neuroprotective microglia, we regarded IL-4-induced microglia expressing *Mrc1* and *Arg1* genes as "M2 microglia," which is widely accepted. In either case, our results demonstrate that M2 type microglia themselves may underlie favorable outcomes in SCI.

With regard to cell transplantation for SCI, previous attempts using various types of stem cells including induced pluripotent stem cells, neural stem cells, embryonic stem cells, and mesenchymal stem cells have induced characteristic effects.[8–15] Our therapeutic approach using microglia mitigates concerns of carcinogenesis and transdifferentiation to unexpected phenotypes in stem cells.[45,46] Although several reports describe the effects of transplantation of primary microglia,[39,47–49] these studies used lipopolysaccharide (LPS)-activated or non-selective microglia, but not M2 microglia. It should be noted that M1 and M2 phenotypes play diverse functions and cannot simply be classified as beneficial or detrimental. Indeed, M1-type microglia have been involved in clearance of damaged and degenerating tissues.[25,37,50] However, M1 microglia are known to have both a detrimental side that causes neurological damage and beneficial aspects such as removing foreign bodies and helping to regenerate myelin.[51,52] In this study, we performed selective M2 microglial transplantation distinct from previous reports; this brought about better effects than those for M1 microglial transplantation. However, M2 was inferior to M1 microglia in migration and phagocytosis in our results as previously described.[53–55] Therefore, it is thought that M1 microglia probably contribute to clearance of debris by phagocytosis after SCI, and the therapeutic effects may be enacted by both M2 and M1 microglia. This insight is suggested by the results that the mRNA expression level of *Cd86* was not significantly different between M1 and M2 groups. Namely, the addition of M2 microglia while maintaining the beneficial side of M1 microglia seems to be important for therapeutic effects in SCI.

To our knowledge, selective M2 microglial transplantation has never been reported in the context of treatment for SCI, although the effect of intravenous systemic administration of bone marrow-derived M2 macrophages for SCI has been reported.[56] Compared with our study, systemic intravenous administration is less invasive than direct transplantation; however, the effect was more efficient in our study because we used only 10^5 M2 microglial cells for transplantation compared with 10^7 M2 macrophages used in systemic intravenous administration.[56] For other neurological diseases, M2 microglia transplantation has been performed in Alzheimer's disease and stroke models.[57,58] M2 microglial transplantation improved cognitive impairment in a rat model of Alzheimer's disease[57] and promoted axonal outgrowth and angiogenesis in a rat model of stroke.[58] This literature described that endogenous microglial polarization to M2 phenotype resulted in improvement of neuronal function.[57] It is explained that the secretion of remodeling factors from transplanted microglia is involved in the recovery of neuronal function, because transplanted microglia were not observed at 21 days after transplantation in the ischemic lesion of the mouse stroke model.[58] These insights agree with our results. The number of transplanted microglia labeled with GFP in the spinal cord considerably decreased 4 weeks after SCI; however, the treatment effects at 4 weeks were confirmed, and *Mrc1* and *Arg1* expressions were higher in the M2 transplanted group. Therefore, selective M2 microglial transplantation has potential as a new therapeutic strategy for neurological diseases, presumably because of the secretion of neuroprotective molecules.

To evaluate whether M2 microglia promoted recovery of motor function in SCI, we analyzed axonal transportation. Positive retrograde axonal transport tracer[59] staining from the hamstrings was observed at proximal levels of the injured site (Th13 level) only in the M2 group. In general, the level of the spinal cord innervating the hamstrings is mainly L2-L4,[60] so the tracer was thought to originate from L2-L4 levels through ascending intraspinal axonal transportation. This result showed that improvement of axonal transportation occurred in the M2 group. In previous reports, IGF1 was reported

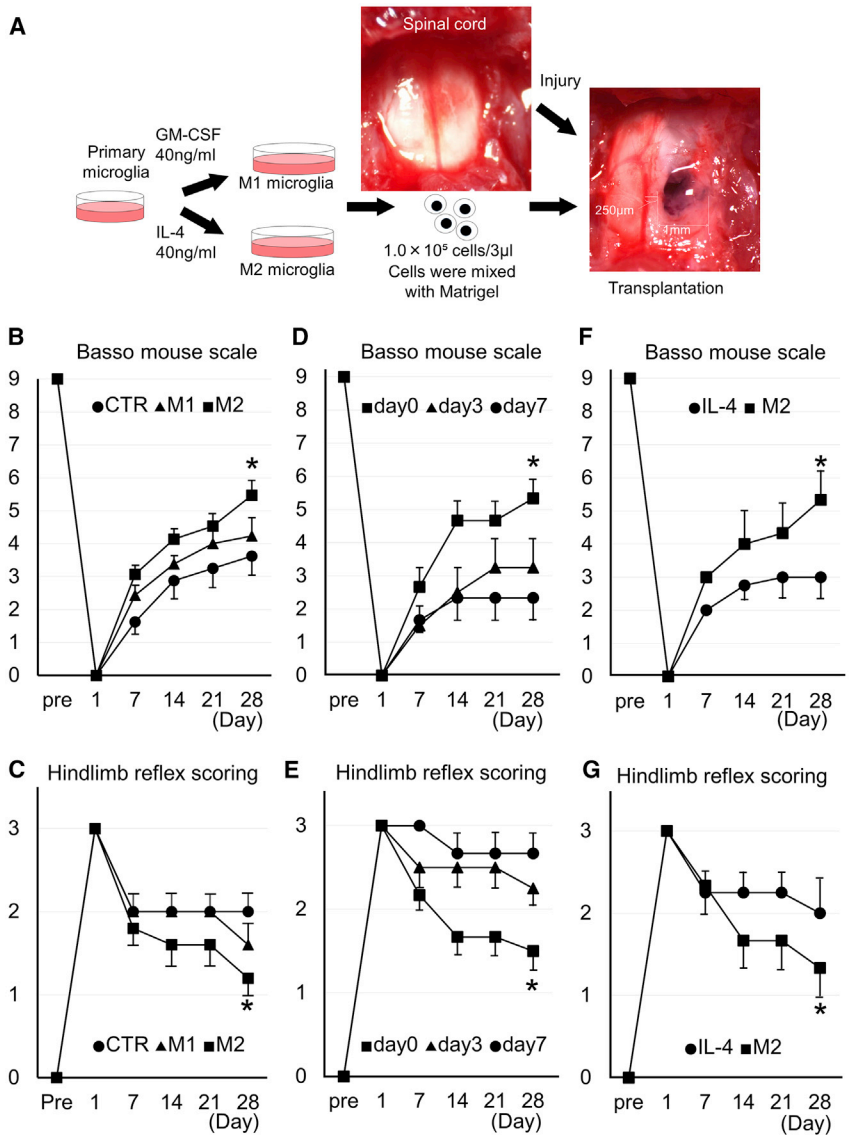

Figure 5. Schematic Procedures and Motor Function at M2 Microglia Transplantation Therapy in the SCI Mouse Model

(A) Schematic procedures of mouse SCI and M1 or M2 microglia transplantation therapy. After exposing the spinal cord (upper middle image), 1-mm circle and 1-mm-depth injury was made at the right side of the mouse spinal cord by a 1-mm-diameter skin biopsy puncher (right panel). A total of 1.0×10^5 M1 or M2 microglia cells (incubated with GM-CSF or IL-4) were transplanted with Matrigel at 3 μL volume into the injured spinal cord (right panel). (B) Time course of the Basso mouse scale in SCI mice after transplantation of Matrigel only (CTR) or M1 or M2 microglia with Matrigel from pre-injury (Pre) to day 28 after injury. Bars showed means ± SEM (n = 9–15 in each group). (C) Time course of the hindlimb reflex scoring in SCI mice after transplantation of Matrigel only (CTR) or M1 or M2 microglia with Matrigel from pre-injury (Pre) to day 28 after injury. Bars showed means ± SEM (n = 5 in each group). (D and E) Time course of the Basso mouse scale (D) and time course of the hindlimb reflex scoring (E) in SCI mice after transplantation of M2 microglia on day 0, 3, or 7 after injury. Bars showed means ± SEM (n = 5–7 in each group). (F and G) Time course of the Basso mouse scale (F) and time course of the hindlimb reflex scoring (G) in SCI mice after transplantation of M2 microglia or in that with systemic injection therapy of IL-4 from pre-injury (Pre) to day 28 after injury. Bars showed means ± SEM (n = 5–7 in each group). *$p < 0.05$ compared with other groups by two-way ANOVA and Scheffe's test. CTR, no cell administered (Matrigel only) group.

to promote axonal regeneration and sprouting in the CNS[61–63] and to improve regeneration of the corticospinal tract in SCI mice.[64] M2 microglia were reported to enhance IGF1 release to assist the resolution of inflammation and promote neuronal survival.[61] In the present study, upregulation of the M2 microglial markers (*Arg1*, *Mrc1*) was confirmed, and *Igf1* expression was also elevated in the spinal cord of M2-transplanted SCI mice. Therefore, IGF1 may contribute to the positive effects of M2 microglia in axonal transportation and recovery of motor function.

A limitation of this study is that we used an uncommon SCI model compared with a conventional spinal cord contusion or resection. We use this protocol, which allowed us to evaluate the histological change in the injured and transplanted area of the spinal cord. We documented the elevation of CD206 in the spinal cord in the M2 group mice at 4 weeks. Understandably, our results should not be applied directly to previous studies that used different SCI models.[39–42] Therefore, we compared M2 microglia transplantation with systemic injection of IL-4 in this study. Transplantation of microglia showed better outcome than IL-4 injection in our SCI model. We also employed experiments in the several timings of administration of M2 cells post-SCI. The treatment effect was most evident in the group in which transplantation was performed immediately after injury. In the clinical scene, motor dysfunction could occur after resection of intramedullary spinal cord tumor. In such cases, it would be possible to apply M2 microglia to the resected site, because it would be similar to our SCI model. We therefore believe that this model deserves attention in the clinical settings such as transplantation therapy after spinal cord surgery.

In the CNS, astrocyte has an important role in physiological and pathological conditions. Notably, astrocyte and microglia are known to regulate each other's phenotypes.[65,66] However, we observed no significant difference in GFAP staining after transplantation of M2 microglia. GLT-1 staining, which is related to the outcome of SCI,[67] also showed no change between the groups. In our model, we could not detect the contribution of the astrocyte, which might be influenced by the animal model.

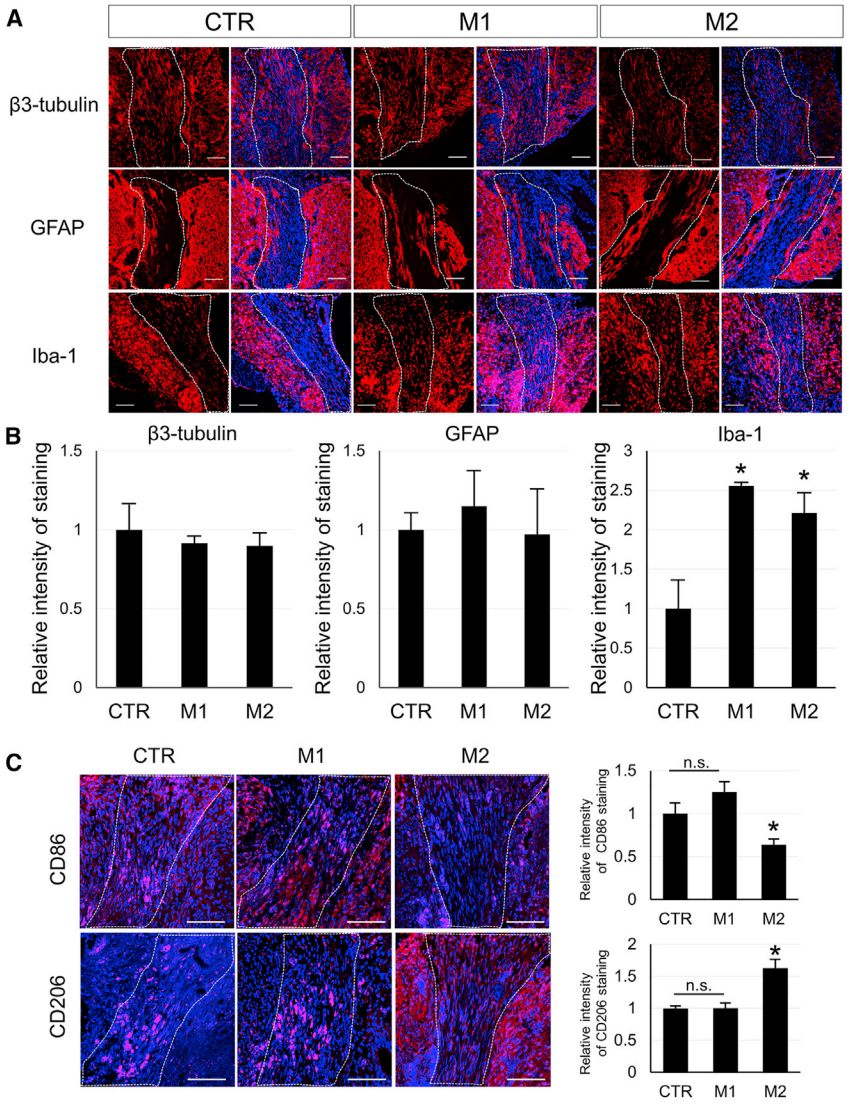

Figure 6. Histological Analysis of Spinal Cords after Injury and Cell Transplantation in SCI Mice

(A) Immunohistochemistry of spinal cord with β3-tubulin (as a neuron marker: red), GFAP (as an astrocyte marker: red), or Iba-1 antibody (as a microglia marker: red) were shown in Matrigel only (CTR) or M1 or M2 microglia with the Matrigel group 4 weeks after SCI and cell transplantation therapy. Blue showed DAPI stain in nuclei. The broken line areas showed the SCI and the transplanted lesion. (B) Each graph showed the relative fluorescence intensity of β3-tubulin, GFAP, or Iba-1 staining within the transplanted area in M1 or M2 group mice against in the CTR group. Error bars showed means + SD (n = 3 in each group). *$p < 0.05$ compared with the CTR group. (C) Immunohistochemistry of spinal cord with CD86 (as an M1 microglia marker: red) or CD206 antibody (as an M2 microglia marker: red) was shown in Matrigel only (CTR) or M1 or M2 microglia with Matrigel group 4 weeks after SCI and cell transplantation therapy. Blue showed DAPI stain in nuclei. The broken line areas showed the SCI and the transplanted lesion. Graph showed the relative fluorescence intensity of CD86 or CD206 staining within the transplanted area in the M1 or M2 group against in the CTR group. Error bars showed means + SD (n = 3 in each group). Scale bar, 100 μm. *$p < 0.05$ compared with other groups. n.s., not significant.

Considering human therapy by M2 microglia, it would be difficult to prepare enough of the primary microglia from human tissues, which await future technology. Rather, it could be possible to differentiate somatic stem cells or induced pluripotent stem cells (iPSCs) to M2 microglia-like cells in the near future.

In conclusion, we have developed a novel cell transplantation therapy for SCI using selectively induced M2 microglia. This therapeutic effect of M2 milieu was evident relative to that of M1 microglia. Considering the availability of autologous transplantation, selective M2 microglia will be a powerful therapeutic option for SCI.

MATERIALS AND METHODS

Animals

All animal experimental protocols were approved by the Institutional Animal Care and Usage Committee (IACUC), Shiga University of Medical Science, and were performed in accordance to the guidelines of the IACUC.

Primary Microglia Isolation and Culture

Primary microglia were prepared as follows.[68] C57BL6/J neonatal mice on the first day of birth were purchased from the Jackson Laboratory through Charles River Laboratories Japan. The mice were decapitated, and their brains were removed by cutting the skull with ophthalmic scissors. Only the cerebral cortex was isolated from the brain using tweezers or scissors, chopped with a scalpel, and treated with 0.25% trypsin-EDTA (Life Technologies, Carlsbad, CA, USA) at 37°C for 10 min. DNase (TAKARA BIO, Kusatsu, Japan) was added to the tissues, which were pipetted thoroughly and centrifuged. The pellet was suspended with culture medium, DMEM/Ham's F-12 (D-MEM/F12) with L-glutamine and phenol red (Wako, Osaka, Japan), supplemented with 10% fetal bovine serum (FBS) (Moregate Biotech, Bulimba, Australia) and 100 U/mL penicillin-streptomycin (Wako, Osaka, Japan), and filtered using a 100-μm cell strainer (Corning, New York, NY, USA). Cells were then seeded on a flask and cultured in a 5% CO_2 incubator at 37°C.

After 14 days of primary cultivation, microglial cells were collected by shaking and re-plating, and were allowed to attach to the substrate for 60–120 min. After checking cell adhesion, the culture medium was changed to culture media containing mouse recombinant GM-CSF at 20 or 40 ng/mL (Wako, Osaka, Japan) or mouse recombinant IL-4 at 20 or 40 ng/mL (Wako, Osaka, Japan) and was cultured for 3 days.

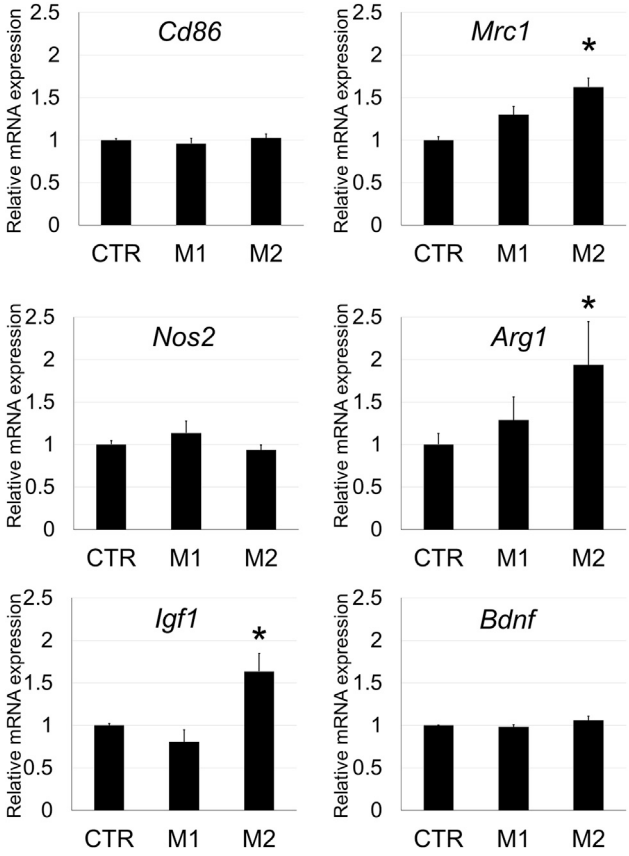

Figure 7. Analysis of mRNA Gene Expression in the Spinal Cord in SCI Mice from Matrigel Only (CTR) or M1 or M2 Microglia with Matrigel Group 4 Weeks after Injury

Bar graphs show the relative mRNA expression of *Cd86*, *Mrc1*, *Nos2*, *Arg1*, *Igf1*, and *Bdnf* in the spinal cord at the injured level (L1) from M1 and M2 groups compared with CTR groups. All of these mRNA expressions were normalized to that of *β-actin*. Error bar showed means + SD (n = 3–4 in each group). *p < 0.05 as compared with each CTR group.

Assessment of Proliferation and Migration of Microglia

Microglia isolated from the primary culture were seeded on a 48-well plate at 6×10^2 cells/well and cultured for 3 days in a culture medium DMEM/F12, supplemented with 1% FBS and the cytokine. The cultured cells were observed under an optical microscope on the first and third days, and the cell number was visually counted in more than five wells per group.

After 3 days, the monolayer of microglia was carefully scraped in a straight line to create a "scratch" with a p200 pipette tip and observed under an optical microscope. An approximately similar area was scraped at the bottom of the dishes. After scratching, these cells were cultured at 37°C in a CO_2 incubator for 24 h, and images were taken at a minimum of three places in each well of culture dishes. The number of cells migrating to the scratched area was visually counted at over five wells per group.

Phagocytosis Assay

Microglia were cultured for 3 days in DMEM/F12 with 10% FBS containing GM-CSF (40 ng/mL) or IL-4 (40 ng/mL) or buffer control. A phagocytosis assay was performed by Latex Bead-Rabbit IgG-Fluorescein isothiocyanate (FITC) complexes (Cayman Chemical, Ann Arbor, MI, USA) according to the manufacturer's protocol. Latex Bead-Rabbit IgG FITC complexes were added to the culture medium, and microglia were incubated for 3 h at 37°C in a CO_2 incubator. After incubation, cells were washed with 0.1 M PBS three times, and photographs were obtained using a fluorescence microscope for five wells per group. FITC intensity in the cell area was measured after subtracting the background value by ImageJ (v.1.52h; NIH, Bethesda, MD, USA).

In Vitro Immunostaining

Microglia isolated from primary culture were seeded on a 48-well plate and cultured for 3 days in DMEM/F12 with 1% FBS and each cytokine. The culture medium was then removed, and the cells were fixed with 4% paraformaldehyde (PFA) in 0.1 M PBS at room temperature for 10 min. After fixing, the cells were incubated with rabbit anti-CD86 antibody (1:1,000; Abcam, Cambridge, UK) or rabbit anti-CD206 antibody (1:1,000; Abcam, Cambridge, UK) as primary antibodies overnight at 4°C. Next, the cells were incubated with anti-rabbit Alexa 488 (1:1,000; Life Technologies, Carlsbad, CA, USA) as a secondary antibody at room temperature for 4 h. After Hoechst dye 33342 (Sigma-Aldrich, St. Louis, MO, USA) staining, they were observed with a laser microscope (FV1000-D; Olympus, Tokyo, Japan). After confirmation of nuclei by Hoechst dye staining, the number of CD86- or CD206-positive cells was visually counted for three wells per group, and the percentage of positive cells was calculated.

In Vitro Gene Expression Analysis

Microglia isolated from primary culture were seeded on a 12-well plate and cultured for 3 days in DMEM/F12 supplemented with 1% FBS and each cytokine. After 3 days, total RNA was extracted from each well according to the RNeasy kit protocol (QIAGEN, Valencia, CA, USA). Using the extracted RNA, reverse transcription was performed with TAKARA PrimeScript RT reagent Kit (TAKARA BIO, Kusatsu, Japan). Real-time PCR was performed using LightCycler 480 SYBR Green I Master (Roche Diagnostics, Manheim, Germany) with LightCycler 480 (Roche Diagnostics, Manheim, Germany) according to each manufacturer's protocol. The following primers were used: *Cd86*, forward primer, 5′-CACGAGCTTTGACAGGAACA-3′ and reverse primer, 5′-TTAGGTTTCGGGTGACCTTG-3′; *Mrc1*, forward primer, 5′-CTATGCAGGCCACTGCTACA-3′ and reverse primer, 5′-GTTCTCATGGCTTGGCTCTC-3′; *Nos2*, forward primer, 5′-TTGGAGCGAGTTGTGGATTG-3′ and reverse primer, 5′-GTAGGTGAGGGCTTGGCTGA-3′; *Arg1*, forward primer, 5′-ACCTGCTGGGAAGGAAGAAAAG-3′ and reverse primer, 5′-GTTCCGAAGCAAGCCAAGGT-3′; *β-actin*, forward primer, 5′-CGTGCGTGACATCAAAGAGAA-3′ and reverse primer, 5′-TGGATGCCACAGGATTCCAT-3′. All data were normalized to *β-actin*, and the results were analyzed using LightCycler 480 software, version 1.5 (Roche Diagnostics,

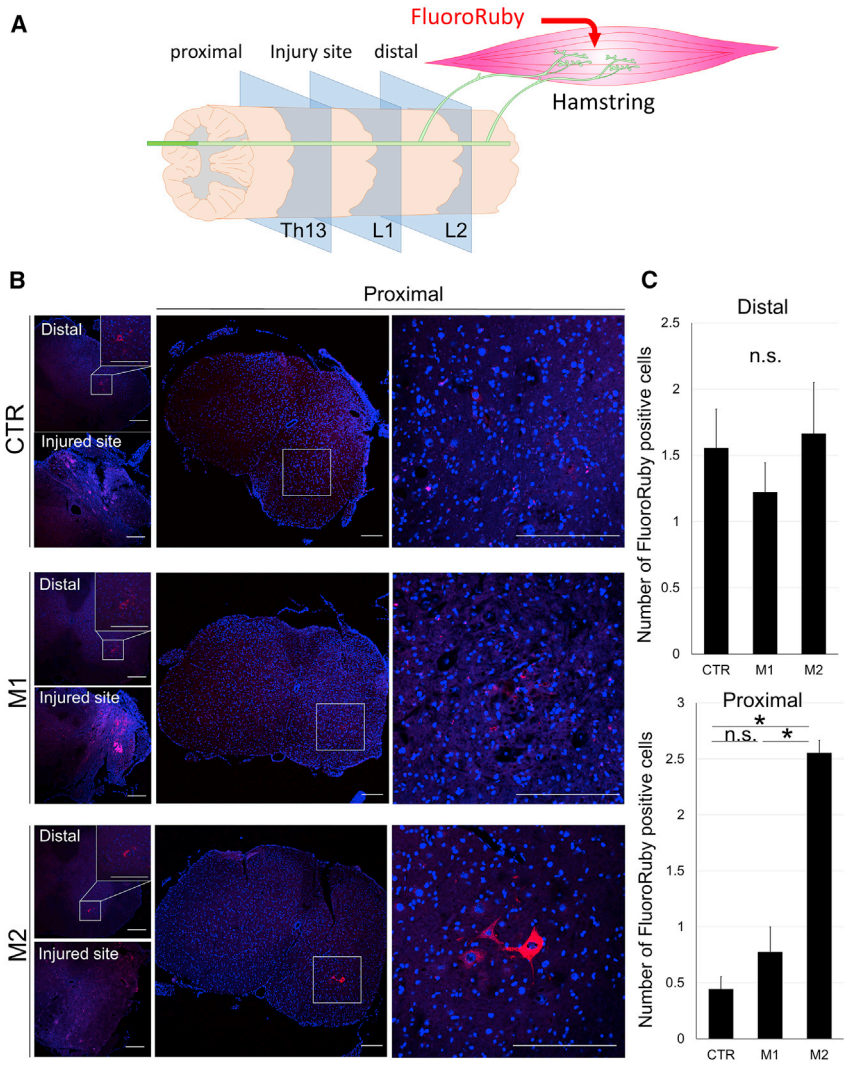

Figure 8. Evaluation of Axonal Transportation by Retrograde Tracer in SCI Mice after Treatment

(A) A schematic diagram of muscle and spinal cord for the experiment of retrograde transportation by FluoroRuby (retrograde tracer). At 5 days after injection of FluoroRuby into the hamstring at the injured side, histological evaluation of spinal cord was performed at the injured site (L1 spinal level) and their proximal (Th13 spinal level) and distal sites (L2 spinal level) in 4-week SCI mice. (B) FluoroRuby stain (red) in spinal cord sections at the injured site and their proximal and distal sites from CTR, M1, and M2 groups. White squares in the distal site (L2 level) show anterior horns in spinal cord sections under low magnification and were enlarged in the right upper corner under high magnification. White squares in the proximal site (Th13 level) show anterior horns in spinal cord sections under low magnification and were enlarged in the right panels under high magnification. Scale bars, 200 μm. (C) Bar graphs show the number of FluoroRuby (FR)-positive neuronal cells per each spinal cord section at distal and proximal sites of injury from CTR, M1, and M2 group mice. Error bars showed means + SD (n = 3 in each group). *p < 0.05. n.s., not significant.

Manheim, Germany). To confirm the reliability of *β-actin* as a housekeeping gene, real-time PCR with each cDNA from all groups was performed using Mouse Housekeeping Gene Primer Set (TAKARA BIO, Kusatsu, Japan). The stability values of housekeeping genes were calculated by BestKeeper software downloaded from BestKeeper-Gene Quantification (available at https://www.gene-quantification.de/bestkeeper.html), and the reliability was evaluated. We have confirmed that the stability value of *β-actin* was appropriate.

In Vivo Cell Therapy in a Mouse Model of SCI

C57BL/6J mice were group housed (three to four animals per cage), maintained on a 12/12-h light/dark cycle at 23°C, and given *ad libitum* access to tap water and standard pellets. Animal care was conducted in accordance to the Guide for Use of Experimental Animals (Shiga University of Medical Science).

Female mice aged 10–14 weeks old were anesthetized. Thoracic spine at level 13 of those mice was identified, and the surrounding skin was disinfected with 70% ethanol. A 1-cm skin incision was made vertically with a scalpel. Next, a scalpel was inserted horizontally into the intervertebral disc of the thoracic spine at levels 12 and 13. Ophthalmic scissors were carefully inserted into the head from the exposed region to avoid damaging the spinal cord, the vertebrae on both sides were incised, and the spine was turned upward to expose the spinal cord. Then, using a skin biopsy puncher with a diameter of 1 mm (Kai Industries, Seki, Japan), a punch of 1-mm depth was made to the exposed spinal cord 250 μm right from the midline. The tissue remaining in the punched area was manually removed using ophthalmic scissors or tweezers. Next, 3 μL of Matrigel (Corning, New York, NY, USA) including cultured M1 or M2 microglia (1.0×10^5 cells/3 μL) or control culture (CTR) was injected into the punched area using a p200 pipette. After confirmation of Matrigel solidification, the spine was manually restored, and subcutaneous tissues on the head and caudal side were loosely sutured with 6-0 nylon to fix the spine. Skin was sutured with a 5-0 nylon. Monoplegia in the right leg was confirmed in all mice the day after transplantation. The effects of microglial transplantation were compared with those of IL-4 systemic intraperitoneal injection (0.35 μg/kg) administered every 12 h for 4 weeks. Microglia transplantation to the spinal cord was performed at day 0, 3, or 7 after SCI, and the effects were compared among the three.

Analysis for the Engraftment of Transplanted Microglia in the SCI Mice Model

To examine the engraftment of the administered microglia, we used the primary microglia isolated from GFP-positive neonatal mice

[C57BL/6-Tg(UBC-GFP)$^{30Scha/J}$], purchased from The Jackson Laboratory (Bar Harbor, ME, USA), for transplantation. Microglia were cultured as mentioned previously. Transplantation of GFP-positive M1 or M2 microglia to SCI mice was also performed as mentioned above. They were sacrificed and fixed with 4% PFA on day 7, 14, or 28 after transplantation. The 10-μm sections of the spinal cord were prepared, and GFP-positive cells were counted in both M1 and M2 groups.

Behavioral Analysis

Motor function of the spinal cord in injured mice was evaluated by BMS for locomotion and hindlimb reflex scoring.[69] For BMS, mice were placed in an open field (LimeLight, Neuroscience, Tokyo, Japan) and observed for over 4 min. As scoring criteria for the hindlimb reflex score, mice were suspended by the tail at a height of approximately 30 cm for 14 s. Posture was scored according to the following criteria: 0, normal; 1, failure to stretch hindlimbs; 2, hindlimb clasping; and 3, hindlimb paralysis. Each assessment was performed pre-transplantation and after transplantation at day 1 and weeks 1, 2, 3, and 4. All behavioral assessments of the animals were performed with the evaluator blinded.

Immunohistochemistry

At 4 weeks after SCI and treatment, spinal cord was isolated after transcardial perfusion with 4% PFA in 0.1 M PBS. Sections of the spinal cord were prepared with a cryostat at 10-μm thickness. For immunostaining, sections were incubated with a primary antibody (rabbit anti-β3-tubulin [Cell Signaling Technology, MA, USA], rabbit anti-Iba-1 [Wako, Osaka, Japan], rabbit anti-GFAP [Cell Signaling Technology, MA, USA], rabbit anti-CD86 [Abcam, Cambridge, UK], rabbit anti-CD206 [Abcam, Cambridge, UK], or rabbit anti-GLT-1 [Cell Signaling Technology, MA, USA]) at 4°C overnight. Then, the sections were incubated with a secondary antibody (goat anti-rabbit Alexa 555 [Life Technologies, Carlsbad, CA, USA]) at room temperature for 4 h. The sections were then mounted with VECTASHIELD containing DAPI (Vector Laboratories, Burlingame, CA, USA). Five sections with a 50-μm interval per each sample were observed using confocal laser microscopy (FV1000-D; Olympus, Tokyo, Japan) to evaluate the data stereologically. The region of interest (ROI) was decided by regarding the high accumulation area of DAPI-positive cells as the injury and transplantation sites. The fluorescence intensity of Alexa 555 in the injured area was measured, and background value was subtracted by ImageJ (v.1.52h; NIH, Bethesda, MD, USA).

In Vivo mRNA Expression Analysis

At 4 weeks after SCI and treatment, the spinal cord was isolated after removal of blood. Total RNA was extracted from the spinal cord using RNeasy kit (QIAGEN, Valencia, CA, USA) according to the manufacturer's protocol. After extraction of RNA, reverse transcription and real-time PCR were performed using TAKARA PrimeScript RT reagent Kit (TAKARA BIO, Kusatsu, Japan), LightCycler 480 SYBR Green I Master (Roche Diagnostics, Manheim, Germany), and LightCycler 480 (Roche Diagnostics, Manheim, Germany) according to each manufacturer's protocol. The following primers were used (details for *Cd86*, *Mrc1*, *Nos2*, *Arg1*, and *β-actin* are shown in "In Vitro Gene Expression Analysis"): *Igf1*, forward primer, 5′-CTGAGCTGGTGGATGCTCT-3′ and reverse primer, 5′-CACTC ATCCACAATGCCTGT-3′; *Bdnf*, forward primer, 5′-TTGTTTTG TGCCGTTTACCA-3′ and reverse primer, 5′-GGTAAGAGAGC CAGCCACTG-3′. We confirmed that *β-actin* is an appropriate housekeeping gene based on the evaluation of the stability value with cDNA from all groups as described in "In Vitro Gene Expression Analysis."

Analysis of Axonal Transportation

At 4 weeks after SCI and treatment, FluoroRuby (Fluorochrome, Denver, CO, USA) was administered at five sites of the right side hamstring with pressure injection using a Hamilton syringe with 30G needle as previously described.[70] Five days after FluoroRuby injection, mice were sacrificed and fixed with 4% PFA. The spinal cord was isolated, and 10-μm sections of spinal cord were prepared with a cryostat at the injured site, as well as 500 μm proximal and distal from the injured lesion. The samples were mounted with VECTASHIELD containing DAPI and were observed under confocal laser microscopy (FV1000-D; Olympus, Tokyo, Japan). The number of FluoroRuby-positive cells was quantified in five sections per sample.

Statistical Analysis

Data are expressed as means ± SD or ± SEM. For most multiple datasets, one-way ANOVA and Scheffe's tests were used. For behavioral analysis, datasets were analyzed by two-way ANOVA and Scheffe's tests. All statistical analyses were performed using IBM SPSS Statistics version 25 (International Business Machines Corporation, Armonk, NY, USA).

SUPPLEMENTAL INFORMATION

Supplemental Information can be found online at https://doi.org/10.1016/j.ymthe.2019.09.004.

AUTHOR CONTRIBUTIONS

S.K. performed the experiments, statistically analyzed the data, and drafted the manuscript. T.T. advised on the experimental procedures, designed the study, and helped to draft and revise the manuscript. M.K. and Y.N. helped to perform the experiments. H.K., Y.S., M.U., and J.O. advised on experimental design and techniques, and provided expertise and feedback. All authors have read and approved the final manuscript.

CONFLICTS OF INTEREST

The authors declare no competing interests.

ACKNOWLEDGMENTS

We would like to thank the providers of technical support of this work with the Central Research Laboratory Shiga University of Medical Science. This work was supported by the Ministry of Education, Culture, Sports, Science and Technology (MEXT) KAKENHI grant numbers JP17H04358 and JP18K07498.

REFERENCES

1. James, S.L., Theadom, A., Ellenbogen, R.G., Bannick, M.S., Montjoy-Venning, W., Lucchesi, L.R., et al.; GBD 2016 Traumatic Brain Injury and Spinal Cord Injury Collaborators (2019). Global, regional, and national burden of traumatic brain injury and spinal cord injury, 1990-2016: a systematic analysis for the Global Burden of Disease Study 2016. Lancet Neurol. *18*, 56–87.
2. Jain, N.B., Ayers, G.D., Peterson, E.N., Harris, M.B., Morse, L., O'Connor, K.C., and Garshick, E. (2015). Traumatic spinal cord injury in the United States, 1993-2012. JAMA *313*, 2236–2243.
3. Hall, O.T., McGrath, R.P., Peterson, M.D., Chadd, E.H., DeVivo, M.J., Heinemann, A.W., and Kalpakjian, C.Z. (2019). The Burden of Traumatic Spinal Cord Injury in the United States: Disability-Adjusted Life Years. Arch. Phys. Med. Rehabil. *100*, 95–100.
4. Devivo, M.J. (2012). Epidemiology of traumatic spinal cord injury: trends and future implications. Spinal Cord *50*, 365–372.
5. Bragge, P., Chau, M., Pitt, V.J., Bayley, M.T., Eng, J.J., Teasell, R.W., Wolfe, D.L., and Gruen, R.L. (2012). An overview of published research about the acute care and rehabilitation of traumatic brain injured and spinal cord injured patients. J. Neurotrauma *29*, 1539–1547.
6. van Middendorp, J.J., Goss, B., Urquhart, S., Atresh, S., Williams, R.P., and Schuetz, M. (2011). Diagnosis and prognosis of traumatic spinal cord injury. Global Spine J. *1*, 1–8.
7. Suzuki, Y., Ishikawa, N., Omae, K., Hirai, T., Ohnishi, K., Nakano, N., Nishida, H., Nakatani, T., Fukushima, M., and Ide, C. (2014). Bone marrow-derived mononuclear cell transplantation in spinal cord injury patients by lumbar puncture. Restor. Neurol. Neurosci. *32*, 473–482.
8. Nakajima, H., Uchida, K., Guerrero, A.R., Watanabe, S., Sugita, D., Takeura, N., Yoshida, A., Long, G., Wright, K.T., Johnson, W.E., and Baba, H. (2012). Transplantation of mesenchymal stem cells promotes an alternative pathway of macrophage activation and functional recovery after spinal cord injury. J. Neurotrauma *29*, 1614–1625.
9. Fujimoto, Y., Abematsu, M., Falk, A., Tsujimura, K., Sanosaka, T., Juliandi, B., Semi, K., Namihira, M., Komiya, S., Smith, A., and Nakashima, K. (2012). Treatment of a mouse model of spinal cord injury by transplantation of human induced pluripotent stem cell-derived long-term self-renewing neuroepithelial-like stem cells. Stem Cells *30*, 1163–1173.
10. Nutt, S.E., Chang, E.A., Suhr, S.T., Schlosser, L.O., Mondello, S.E., Moritz, C.T., Cibelli, J.B., and Horner, P.J. (2013). Caudalized human iPSC-derived neural progenitor cells produce neurons and glia but fail to restore function in an early chronic spinal cord injury model. Exp. Neurol. *248*, 491–503.
11. Karimi-Abdolrezaee, S., Eftekharpour, E., Wang, J., Morshead, C.M., and Fehlings, M.G. (2006). Delayed transplantation of adult neural precursor cells promotes remyelination and functional neurological recovery after spinal cord injury. J. Neurosci. *26*, 3377–3389.
12. Parr, A.M., Kulbatski, I., Zahir, T., Wang, X., Yue, C., Keating, A., and Tator, C.H. (2008). Transplanted adult spinal cord-derived neural stem/progenitor cells promote early functional recovery after rat spinal cord injury. Neuroscience *155*, 760–770.
13. Lu, P., Wang, Y., Graham, L., McHale, K., Gao, M., Wu, D., Brock, J., Blesch, A., Rosenzweig, E.S., Havton, L.A., et al. (2012). Long-distance growth and connectivity of neural stem cells after severe spinal cord injury. Cell *150*, 1264–1273.
14. Marques, S.A., Almeida, F.M., Fernandes, A.M., dos Santos Souza, C., Cadilhe, D.V., Rehen, S.K., and Martinez, A.M. (2010). Predifferentiated embryonic stem cells promote functional recovery after spinal cord compressive injury. Brain Res. *1349*, 115–128.
15. Wu, S., FitzGerald, K.T., and Giordano, J. (2018). On the viability and potential value of stem cells for repair and treatment of central neurotrauma: Overview and speculations. Front. Neurol. *9*, 602.
16. Anwar, M.A., Al Shehabi, T.S., and Eid, A.H. (2016). Inflammogenesis of Secondary Spinal Cord Injury. Front. Cell. Neurosci. *10*, 98.
17. Oyinbo, C.A. (2011). Secondary injury mechanisms in traumatic spinal cord injury: a nugget of this multiply cascade. Acta Neurobiol. Exp. (Warsz.) *71*, 281–299.
18. Fehlings, M.G., and Nguyen, D.H. (2010). Immunoglobulin G: a potential treatment to attenuate neuroinflammation following spinal cord injury. J. Clin. Immunol. *30* (*Suppl 1*), S109–S112.
19. Zhang, N., Yin, Y., Xu, S.J., Wu, Y.P., and Chen, W.S. (2012). Inflammation & apoptosis in spinal cord injury. Indian J. Med. Res. *135*, 287–296.
20. Saijo, K., and Glass, C.K. (2011). Microglial cell origin and phenotypes in health and disease. Nat. Rev. Immunol. *11*, 775–787.
21. Salter, M.W., and Stevens, B. (2017). Microglia emerge as central players in brain disease. Nat. Med. *23*, 1018–1027.
22. Kabba, J.A., Xu, Y., Christian, H., Ruan, W., Chenai, K., Xiang, Y., Zhang, L., Saavedra, J.M., and Pang, T. (2018). Microglia: Housekeeper of the Central Nervous System. Cell. Mol. Neurobiol. *38*, 53–71.
23. Crain, J.M., Nikodemova, M., and Watters, J.J. (2013). Microglia express distinct M1 and M2 phenotypic markers in the postnatal and adult central nervous system in male and female mice. J. Neurosci. Res. *91*, 1143–1151.
24. Ransohoff, R.M. (2016). A polarizing question: do M1 and M2 microglia exist? Nat. Neurosci. *19*, 987–991.
25. Cherry, J.D., Olschowka, J.A., and O'Banion, M.K. (2014). Neuroinflammation and M2 microglia: the good, the bad, and the inflamed. J. Neuroinflammation *11*, 98.
26. Hegyi, B., Környei, Z., Ferenczi, S., Fekete, R., Kudlik, G., Kovács, K.J., Madarász, E., and Uher, F. (2014). Regulation of mouse microglia activation and effector functions by bone marrow-derived mesenchymal stem cells. Stem Cells Dev. *23*, 2600–2612.
27. Kigerl, K.A., Gensel, J.C., Ankeny, D.P., Alexander, J.K., Donnelly, D.J., and Popovich, P.G. (2009). Identification of two distinct macrophage subsets with divergent effects causing either neurotoxicity or regeneration in the injured mouse spinal cord. J. Neurosci. *29*, 13435–13444.
28. Hamilton, J.A. (2002). GM-CSF in inflammation and autoimmunity. Trends Immunol. *23*, 403–408.
29. Lee, S.C., Liu, W., Brosnan, C.F., and Dickson, D.W. (1994). GM-CSF promotes proliferation of human fetal and adult microglia in primary cultures. Glia *12*, 309–318.
30. Boche, D., Perry, V.H., and Nicoll, J.A.R. (2013). Review: activation patterns of microglia and their identification in the human brain. Neuropathol. Appl. Neurobiol. *39*, 3–18.
31. Pepe, G., De Maglie, M., Minoli, L., Villa, A., Maggi, A., and Vegeto, E. (2017). Selective proliferative response of microglia to alternative polarization signals. J. Neuroinflammation *14*, 236.
32. Varnum, M.M., and Ikezu, T. (2012). The classification of microglial activation phenotypes on neurodegeneration and regeneration in Alzheimer's disease brain. Arch. Immunol. Ther. Exp. (Warsz.) *60*, 251–266.
33. Geloso, M.C., Corvino, V., Marchese, E., Serrano, A., Michetti, F., and D'Ambrosi, N. (2017). The dual role of microglia in ALS: Mechanisms and therapeutic approaches. Front. Aging Neurosci. *9*, 242.
34. Gensel, J.C., and Zhang, B. (2015). Macrophage activation and its role in repair and pathology after spinal cord injury. Brain Res. *1619*, 1–11.
35. Orihuela, R., McPherson, C.A., and Harry, G.J. (2016). Microglial M1/M2 polarization and metabolic states. Br. J. Pharmacol. *173*, 649–665.
36. Cherry, J.D., Olschowka, J.A., and O'Banion, M.K. (2015). Arginase 1+ microglia reduce Aβ plaque deposition during IL-1β-dependent neuroinflammation. J. Neuroinflammation *12*, 203.
37. Tang, Y., and Le, W. (2016). Differential Roles of M1 and M2 Microglia in Neurodegenerative Diseases. Mol. Neurobiol. *53*, 1181–1194.
38. Lewis, K.E., Rasmussen, A.L., Bennett, W., King, A., West, A.K., Chung, R.S., and Chuah, M.I. (2014). Microglia and motor neurons during disease progression in the SOD1G93A mouse model of amyotrophic lateral sclerosis: changes in arginase1 and inducible nitric oxide synthase. J. Neuroinflammation *11*, 55.
39. Marcol, W., Ślusarczyk, W., Larysz-Brysz, M., Łabuzek, K., Kapustka, B., Staszkiewicz, R., Rosicka, P., Kalita, K., Węglarz, W., and Lewin-Kowalik, J. (2017). Extended magnetic resonance imaging studies on the effect of classically activated microglia transplantation on white matter regeneration following spinal cord focal injury in adult rats. Exp. Ther. Med. *14*, 4869–4877.

40. Wang, C., Wang, Q., Lou, Y., Xu, J., Feng, Z., Chen, Y., Tang, Q., Zheng, G., Zhang, Z., Wu, Y., et al. (2018). Salidroside attenuates neuroinflammation and improves functional recovery after spinal cord injury through microglia polarization regulation. J. Cell. Mol. Med. *22*, 1148–1166.

41. Kim, J.H., Kim, J.Y., Mun, C.H., Suh, M., and Lee, J.E. (2017). Agmatine Modulates the Phenotype of Macrophage Acute Phase after Spinal Cord Injury in Rats. Exp. Neurobiol. *26*, 278–286.

42. Lima, R., Monteiro, S., Lopes, J.P., Barradas, P., Vasconcelos, N.L., Gomes, E.D., Assunção-Silva, R.C., Teixeira, F.G., Morais, M., Sousa, N., et al. (2017). Systemic interleukin-4 administration after spinal cord injury modulates inflammation and promotes neuroprotection. Pharmaceuticals (Basel) *10*, e83.

43. Mantovani, A., Sica, A., Sozzani, S., Allavena, P., Vecchi, A., and Locati, M. (2004). The chemokine system in diverse forms of macrophage activation and polarization. Trends Immunol. *25*, 677–686.

44. Napolitano, A., Pellegrini, L., Dey, A., Larson, D., Tanji, M., Flores, E.G., Kendrick, B., Lapid, D., Powers, A., Kanodia, S., et al. (2016). Minimal asbestos exposure in germline BAP1 heterozygous mice is associated with deregulated inflammatory response and increased risk of mesothelioma. Oncogene *35*, 1996–2002.

45. Ji, J., Ng, S.H., Sharma, V., Neculai, D., Hussein, S., Sam, M., Trinh, Q., Church, G.M., McPherson, J.D., Nagy, A., and Batada, N.N. (2012). Elevated coding mutation rate during the reprogramming of human somatic cells into induced pluripotent stem cells. Stem Cells *30*, 435–440.

46. Martino, G., Pluchino, S., Bonfanti, L., and Schwartz, M. (2011). Brain regeneration in physiology and pathology: the immune signature driving therapeutic plasticity of neural stem cells. Physiol. Rev. *91*, 1281–1304.

47. Prewitt, C.M.F., Niesman, I.R., Kane, C.J.M., and Houlé, J.D. (1997). Activated macrophage/microglial cells can promote the regeneration of sensory axons into the injured spinal cord. Exp. Neurol. *148*, 433–443.

48. Kou, D., Li, T., Liu, H., Liu, C., Yin, Y., Wu, X., and Yu, T. (2018). Transplantation of rat-derived microglial cells promotes functional recovery in a rat model of spinal cord injury. Braz. J. Med. Biol. Res. *51*, e7076.

49. Lin, X., Zhao, T., Walker, M., Ding, A., Lin, S., Cao, Y., Zheng, J., Liu, X., Geng, M., Xu, X.M., and Liu, S. (2016). Transplantation of Pro-Oligodendroblasts, Preconditioned by LPS-Stimulated Microglia, Promotes Recovery After Acute Contusive Spinal Cord Injury. Cell Transplant. *25*, 2111–2128.

50. Greenhalgh, A.D., and David, S. (2014). Differences in the phagocytic response of microglia and peripheral macrophages after spinal cord injury and its effects on cell death. J. Neurosci. *34*, 6316–6322.

51. Hanisch, U.K., and Kettenmann, H. (2007). Microglia: active sensor and versatile effector cells in the normal and pathologic brain. Nat. Neurosci. *10*, 1387–1394.

52. Glezer, I., Simard, A.R., and Rivest, S. (2007). Neuroprotective role of the innate immune system by microglia. Neuroscience *147*, 867–883.

53. Schermer, C., and Humpel, C. (2002). Granulocyte macrophage-colony stimulating factor activates microglia in rat cortex organotypic brain slices. Neurosci. Lett. *328*, 180–184.

54. Moreno, J.L., Mikhailenko, I., Tondravi, M.M., and Keegan, A.D. (2007). IL-4 promotes the formation of multinucleated giant cells from macrophage precursors by a STAT6-dependent, homotypic mechanism: contribution of E-cadherin. J. Leukoc. Biol. *82*, 1542–1553.

55. von Zahn, J., Möller, T., Kettenmann, H., and Nolte, C. (1997). Microglial phagocytosis is modulated by pro- and anti-inflammatory cytokines. Neuroreport *8*, 3851–3856.

56. Ma, S.F., Chen, Y.J., Zhang, J.X., Shen, L., Wang, R., Zhou, J.S., Hu, J.G., and Lü, H.Z. (2015). Adoptive transfer of M2 macrophages promotes locomotor recovery in adult rats after spinal cord injury. Brain Behav. Immun. *45*, 157–170.

57. Zhu, D., Yang, N., Liu, Y.Y., Zheng, J., Ji, C., and Zuo, P.P. (2016). M2 Macrophage Transplantation Ameliorates Cognitive Dysfunction in Amyloid-β-Treated Rats Through Regulation of Microglial Polarization. J. Alzheimers Dis. *52*, 483–495.

58. Kanazawa, M., Miura, M., Toriyabe, M., Koyama, M., Hatakeyama, M., Ishikawa, M., Nakajima, T., Onodera, O., Takahashi, T., Nishizawa, M., and Shimohata, T. (2017). Microglia preconditioned by oxygen-glucose deprivation promote functional recovery in ischemic rats. Sci. Rep. *7*, 42582.

59. Schmued, L., Kyriakidis, K., and Heimer, L. (1990). In vivo anterograde and retrograde axonal transport of the fluorescent rhodamine-dextran-amine, Fluoro-Ruby, within the CNS. Brain Res. *526*, 127–134.

60. McHanwell, S., and Biscoe, T.J. (1981). The localization of motoneurons supplying the hindlimb muscles of the mouse. Philos. Trans. R. Soc. Lond. B Biol. Sci. *293*, 477–508.

61. Joshi, Y., Sória, M.G., Quadrato, G., Inak, G., Zhou, L., Hervera, A., Rathore, K.I., Elnaggar, M., Cucchiarini, M., Marine, J.C., et al. (2015). The MDM4/MDM2-p53-IGF1 axis controls axonal regeneration, sprouting and functional recovery after CNS injury. Brain *138*, 1843–1862.

62. Feldman, E.L., Sullivan, K.A., Kim, B., and Russell, J.W. (1997). Insulin-like growth factors regulate neuronal differentiation and survival. Neurobiol. Dis. *4*, 201–214.

63. Özdinler, P.H., and Macklis, J.D. (2006). IGF-I specifically enhances axon outgrowth of corticospinal motor neurons. Nat. Neurosci. *9*, 1371–1381.

64. Liu, Y., Wang, X., Li, W., Zhang, Q., Li, Y., Zhang, Z., Zhu, J., Chen, B., Williams, P.R., Zhang, Y., et al. (2017). A Sensitized IGF1 Treatment Restores Corticospinal Axon-Dependent Functions. Neuron *95*, 817–833.e4.

65. Shinozaki, Y., Shibata, K., Yoshida, K., Shigetomi, E., Gachet, C., Ikenaka, K., Tanaka, K.F., and Koizumi, S. (2017). Transformation of Astrocytes to a Neuroprotective Phenotype by Microglia via $P2Y_1$ Receptor Downregulation. Cell Rep. *19*, 1151–1164.

66. Jha, M.K., Jo, M., Kim, J.H., and Suk, K. (2019). Microglia-Astrocyte Crosstalk: An Intimate Molecular Conversation. Neuroscientist *25*, 227–240.

67. Li, K., Nicaise, C., Sannie, D., Hala, T.J., Javed, E., Parker, J.L., Putatunda, R., Regan, K.A., Suain, V., Brion, J.P., et al. (2014). Overexpression of the astrocyte glutamate transporter GLT1 exacerbates phrenic motor neuron degeneration, diaphragm compromise, and forelimb motor dysfunction following cervical contusion spinal cord injury. J. Neurosci. *34*, 7622–7638.

68. Terashima, T., Nakae, Y., Katagi, M., Okano, J., Suzuki, Y., and Kojima, H. (2018). Stem cell factor induces polarization of microglia to the neuroprotective phenotype *in vitro*. Heliyon *4*, e00837.

69. Basso, D.M., Fisher, L.C., Anderson, A.J., Jakeman, L.B., McTigue, D.M., and Popovich, P.G. (2006). Basso Mouse Scale for locomotion detects differences in recovery after spinal cord injury in five common mouse strains. J. Neurotrauma *23*, 635–659.

70. Mohan, R., Tosolini, A.P., and Morris, R. (2014). Targeting the motor end plates in the mouse hindlimb gives access to a greater number of spinal cord motor neurons: an approach to maximize retrograde transport. Neuroscience *274*, 318–330.